THE JOURNAL OF BIOLOGICAL CHEMISTRY
Vol. 277, No. 34, Issue of August 23, pp. 31048–31055, 2002

Printed in U.S.A.

Role of the N-terminal Transmembrane Region of the Multidrug Resistance Protein MRP2 in Routing to the Apical Membrane in MDCKII Cells*

Received for publication, May 1, 2002, and in revised form, June 10, 2002
Published, JBC Papers in Press, June 11, 2002, DOI 10.1074/jbc.M204267200

Sara B. Mateus Fernández‡§¶, Zsolt Holló‖, Andras Kern‡‡, Éva Bakos‡‡§§, Paul A. Fischer¶¶, Piet Borst‖, and Raymond Evers‡§‖‖**

From the ‡Georg-Speyer-Haus, Paul Ehrlich Strasse 42-44, 60596 Frankfurt a.M., Germany, the ‖Division of Molecular Biology and Center for Biomedical Genetics, Netherlands Cancer Institute, Plesmanlaan 121, 1066 CX Amsterdam, The Netherlands, §§National Institute of Haematology and Immunology, Daroczi u. 24, 1113 Budapest, Hungary, ‡‡Institute of Enzymology, Biological Research Center, Hungarian Academy of Sciences, H-1113 Budapest, Hungary, and the Departments of §Drug Metabolism and ¶¶Atherosclerosis and Endocrinology, Merck, Rahway, New Jersey 07065

In polarized cells, the multidrug resistance protein MRP2 is localized in the apical plasma membrane, whereas MRP1, another multidrug resistance protein (MRP) family member, is localized in the basolateral membrane. MRP1 and MRP2 are thought to contain an N-terminal region of five transmembrane segments (TMD_0) coupled to 2 times six transmembrane segments via an intracellular loop (L_0). We previously demonstrated for MRP1 that a mutant lacking TMD_0 but still containing L_0, called L_0ΔMRP1, was functional and routed to the lateral plasma membrane. To investigate the role of the TMD_0L_0 region of MRP2 in routing to the apical membrane, we generated mutants similar to those made for MRP1. In contrast to L_0ΔMRP1, L_0ΔMRP2 was associated with an intracellular compartment, most likely endosomes. Co-expression with TMD_0, however, resulted in apical localization of L_0ΔMRP2 and transport activity. Uptake experiments with vesicles containing L_0ΔMRP2 demonstrated that the molecule is able to transport LTC_4. An MRP2 mutant without TMD_0L_0, ΔMRP2, was only core-glycosylated and localized intracellularly. Co-expression of ΔMRP2 with TMD_0L_0 resulted in an increased protein level of ΔMRP2, full glycosylation of the protein, routing to the apical membrane, and transport activity. Our results suggest that the TMD_0 region is required for routing to or stable association with the apical membrane.

Several members of the ATP-binding cassette superfamily of transporter proteins are able to confer multidrug resistance to tumor cells. Examples are MDR1 P-glycoprotein (1) and members of the multidrug resistance protein (MRP)[1] family, MRP1 and MRP2 (2, 3). Whereas MDR1 Pgp preferably transports large amphipathic molecules (4), MRP1 and MRP2 transport in addition acidic compounds with a large hydrophobic moiety such as drugs conjugated with glutathione, glucuronide, or sulfate (5–7). MRP1- and MRP2-mediated transport of cytotoxic drugs not known to be conjugated to negatively charged ligands is most likely due to co-transport with reduced glutathione (8–12). Besides MRP1 and MRP2, there are seven other MRP homologs expressed in humans, designated MRP3 to -9 (13–15). MRP3 to -5 can confer resistance against some anticancer drugs and are able to transport certain organic anions (16–21).

The predicted membrane topology of MDR1 Pgp and MRPs is different. Whereas MDR1 Pgp and MRPs share a similar core region consisting of two times six transmembrane regions and two intracellular ATP-binding cassettes, MRP1 and MRP2, and several other members of the MRP family contain an extra amino-terminal domain of about 280 amino acids (22–26) (see also Fig. 1). This latter domain is thought to consist of five transmembrane segments and is bound to the core region via an intracellular loop (L_0) of ~80 amino acids. By producing various mutants of MRP1 in baculovirus-infected insect cells, we and others previously showed that the MRP1 core, called ΔMRP1, was inactive. Co-expression of the core (ΔMRP1) with TMD_0L_0, however, resulted in an active transporter (24, 27). Interestingly, extending the core region with the intracellular loop L_0 alone also resulted in transport activity, indicating that the TMD_0 region is dispensable for the function of MRP1 (27). In a recent report, we demonstrated that co-expression of the L_0 peptide with ΔMRP1 in insect cells resulted in an active transporter, suggesting that L_0 forms a distinct domain within MRP1 that specifically interacts with the core region (28).

In polarized monolayers of Madin-Darby canine kidney (MDCKII) cells, MDR1 Pgp and MRP2 are localized in the apical membrane, whereas MRP1 is found in the lateral membrane (29, 30, 27, 31). Interestingly, the MRP1 molecule containing L_0 but lacking the TMD_0 segment (L_0ΔMRP1), which showed activity in insect cells, was also active in MDCKII cells and routed to the lateral plasma membrane (27).

To examine whether the TMD_0 segment is dispensable for the routing of MRP2 to the apical membrane, we have constructed similar mutants as described above for MRP1. Our results show that the TMD_0 region of MRP2 is required for

* This work was supported in part by Deutsche Forschungsgemeinschaft Grant EV39-1-1 (to R. E.). The costs of publication of this article were defrayed in part by the payment of page charges. This article must therefore be hereby marked "*advertisement*" in accordance with 18 U.S.C. Section 1734 solely to indicate this fact.

¶ Participant in an international research exchange program supported by Merck.

** Recipient of a European Molecular Biology long term fellowship.

‖‖ To whom correspondence should be addressed: Dept. of Drug Metabolism, RY80E-200, Merck, P.O. Box 2000, Rahway, NJ 07065. Tel.: 732-594-0427; Fax: 732-594-8370; E-mail: Raymond_Evers@merck.com.

[1] The abbreviations used are: MRP, human multidrug resistance protein; ALLN, *N*-acetyl-L-leucil-L-leucil-L-norleucinal; ECFP, enhanced cyan fluorescent protein; DNP-GS, dinitrophenyl *S*-glutathione; LTC_4, leukotriene C_4; MDR1, multidrug resistance protein 1; Pgp, P-glycoprotein; mAb, monoclonal antibody; CDNB, 1-chloro-2,4-dinitrobenzene; CFTR, cystic fibrosis transmembrane conductance regulator.

apical routing in MDCKII cells and/or for the stabilization of the protein in the apical plasma membrane, in contrast to what was previously found for MRP1.

EXPERIMENTAL PROCEDURES

Materials—[^{3}H]Vinblastine (9.4 Ci/mmol), inulin-[^{14}C]carboxylic acid (6.4 mCi/mmol; average molecular weight 5175), and [^{14}C]1-chloro-2,4-dinitrobenzene ([^{14}C]CDNB; 10 mCi/mmol) were from Amersham Biosciences. [^{3}H]LTC_4 (135 Ci/mmol) was from PerkinElmer Life Sciences. Lactacystin and *N*-acetyl-L-leucil-L-leucil-L-norleucinal (ALLN) were from Calbiochem, and tunicamycin was from Sigma (Deisenhofen, Germany). pECFP-Endo and pECFP-Golgi vectors were from CLONTECH. Alexa Fluor 532 goat anti-mouse Ig (H + L) conjugate was from Molecular Probes, Inc. (Eugene, OR). Fluorescein isothiocyanate-labeled sheep anti-mouse IgG was from Chemicon International, Inc. (Temecula, CA).

Generation of MRP2 Variants and Their Expression in MDCKII Cells—All MRP2 (ABCC2) mutants used in this study (see Fig. 1) were generated by PCR using the human MRP2 sequence as the template (32) (GenBank™ accession number U49248). The HA-TMD_0 fragment encompasses amino acids 2–189 with a hemagglutinin tag (amino acids MAYPYDVPDYA) fused to the amino terminus. TMD_0L_0 encompasses amino acids 1–305, ΔMRP2 represents amino acids 306–1545, and L_0ΔMRP2 represents amino acids 189–1545. PCR fragments were verified by sequence analysis. Further details are available upon request. MRP2, ΔMRP2, and L_0ΔMRP2 were inserted into the retroviral vector pCMV-neo (33); HA-TMD_0 and TMD_0L_0 were inserted into the retroviral vector pBabe-CMV-Puro (kindly provided by Dr. J. Wijnholds, Netherlands Cancer Institute, Amsterdam, The Netherlands; see also Bakos *et al.* (28)). Retroviral transductions of MDCKII cells were performed as described previously (30). After selection of transduced cells with either G418 (800 μg/ml) or puromycin (2 μg/ml), single clones were isolated. Detection of the various mutant MRP2 molecules was performed by Western blotting. Proteins were detected using the appropriate monoclonal antibodies (mAbs) (see Fig. 2*A*).

Expression of MRP2 and L_0ΔMRP2 in Insect Cells and Vesicle Uptake Experiments—L_0ΔMRP2 cDNAs were removed from the pCMV-L_0ΔMRP2 construct and subcloned into the pAcUW21 plasmid (Invitrogen). pAcUW21-MRP2 was described previously (28). Recombinant baculovirus was prepared and cultured as described by Bakos *et al.* (27) by using the BaculoGold transfection kit (Pharmingen, San Diego, CA). [^{3}H]LTC_4 uptake experiments were performed as described previously (27).

Immunocytochemistry—Cells were grown on microporous polycarbonate membrane filters (3-μm pore size, 24-mm diameter, Transwell™ 3414; Corning Costar Corp., Cambridge, MA) at a density of 5×10^5 cells/well as described previously (30). Antibody incubations were as described previously (30). Cells were examined with a Leica TCS SP confocal laser-scanning microscope (Leica Microsystems Heidelberg GmbH, Mannheim, Germany) equipped with a ×63 objective. For the co-localization experiments (see Fig. 7), cells were examined with a Zeiss Laser-Scanning Microscope LSM410 equipped with a ×40 objective. Enhanced cyan fluorescent protein (ECFP) was excited with a krypton 413 laser line; Alexa 532 was excited with a HeNe 543 laser line.

Transfection of pECFP Vectors in MDCKII Cells—MDCKII-MRP2 and MDCKII-L_0ΔMRP2 cells were seeded in 12-well plates (3-μm pore size, 12-mm diameter, Transwell™ 3402; Corning Costar Corp., Cambridge, MA) at a density of 1.5×10^5 cells/well. The next day, cells were transiently transfected with pECFP-Endo (0.8 g) or pECFP-Golgi (1.25 g) using LipofectAMINE™ 2000 reagent (Invitrogen) according to the instructions of the manufacturer. Five hours after the transfection, the medium was replaced with Dulbecco's modified Eagle's medium. Cells were analyzed after culturing for 24 h. Longer incubation times resulted in toxic effects of the pECFP vectors.

Transport Assays with MDCKII Cells—Cells were grown for 3 days on microporous polycarbonate filters at a density of 2×10^6 cells/well. Export of [^{14}C]dinitrophenyl glutathione ([^{14}C]DNP-GS) from cells was determined by incubating cells with [^{14}C]CDNB as described previously (30). [^{3}H]Vinblastine transport assays were carried out exactly as described (30).

Deglycosylation Experiments and Treatment with Proteasome Inhibitors—Cells were seeded in Petri dishes and grown overnight. The next day, tunicamycin (1.5 μg/ml) was added to the medium, and cells were harvested at the time points indicated. For treatment with proteasome inhibitors, cells were seeded as mentioned above. The next day, lactacystin (50 μM) or ALLN (50 μg/ml) was added to the medium. Cells were harvested after an incubation time of 8 h.

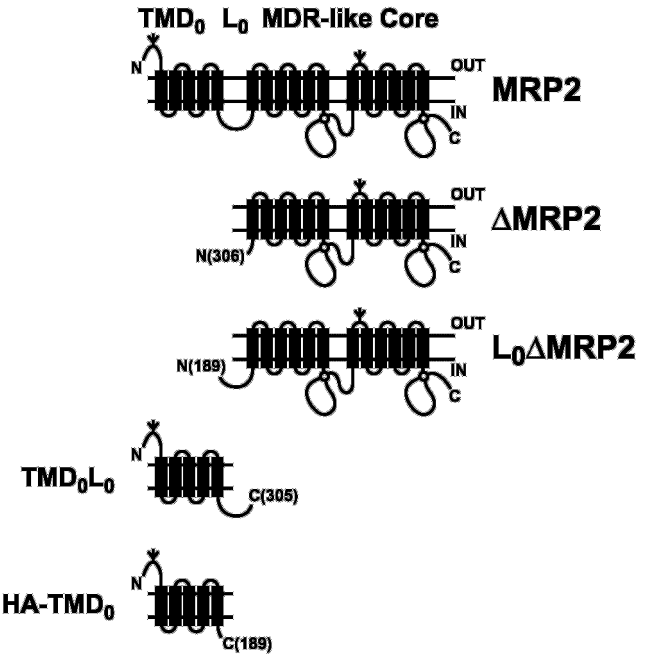

FIG. 1. **Schematic representation of the MRP2 mutants used in this study.** Putative glycosylation sites are indicated by branched motifs.

RESULTS

Generation of MDCKII Cells Expressing MRP2 Constructs—To investigate the role of the TMD_0L_0 segment in the routing and function of MRP2, the following mutants were generated (Fig. 1): (i) ΔMRP2 (amino acids 306–1545), (ii) HA-TMD_0 (HA tag followed by amino acids 2–189), (iii) TMD_0L_0 (amino acids 1–305), and (iv) L_0ΔMRP2 (amino acids 189–1545). The TMD_0L_0 and TMD_0 fragments were cloned into the retroviral pBabe-CMV-puro vector. ΔMRP2 and L_0ΔMRP2 were cloned into the pCMV-neo vector. The use of the pBabe-CMV-Puro and pCMV-neo vectors enabled the selection of two different constructs in one cell. The ΔMRP2 and L_0ΔMRP2 proteins were detected with mAb M_2III-6, TMD_0L_0 and L_0ΔMRP2 were detected with mAb M_2I-4, and HA-TMD_0 was detected with mAb 12CA5 (recognizing the HA epitope), as shown in Fig. 2*A*. Monoclonal antibody M_2III-6 was raised against amino acids 1339–1545 from rat Mrp2 (3) but also recognizes human MRP2 (32); mAb M_2I-4 was raised against amino acids 215–310 of human MRP2 (34).

We previously characterized MDCKII-derived cell lines stably producing the MRP2 protein (30). Using retroviral transductions, we generated MDCKII-derived clones stably expressing the ΔMRP2 or L_0ΔMRP2 constructs. By Western blot analysis, we identified several clones that produced relatively high amounts of L_0ΔMRP2 (Fig. 2*B*, *lane 7*). We also succeeded in isolating clones producing ΔMRP2, but the protein was difficult to detect in total cell lysates (not visible on the exposure of the Western blot shown in Fig. 2*B*, *lane 3*, but see Fig. 3). To investigate whether this was due to proteasome-mediated degradation, cells were incubated in the presence of the proteasome inhibitors ALLN and lactacystin, and this resulted in a clear increase in the amount of ΔMRP2 (Fig. 3).

The MDCKII-MRP2 and MDCKII-L_0ΔMRP2 cells were retrovirally transduced with plasmids containing either TMD_0L_0 or HA-TMD_0. Cells were selected with puromycin, and single clones were analyzed by Western blotting. As documented in Fig. 2, *B* and *C*, clones producing both the ΔMRP2 and

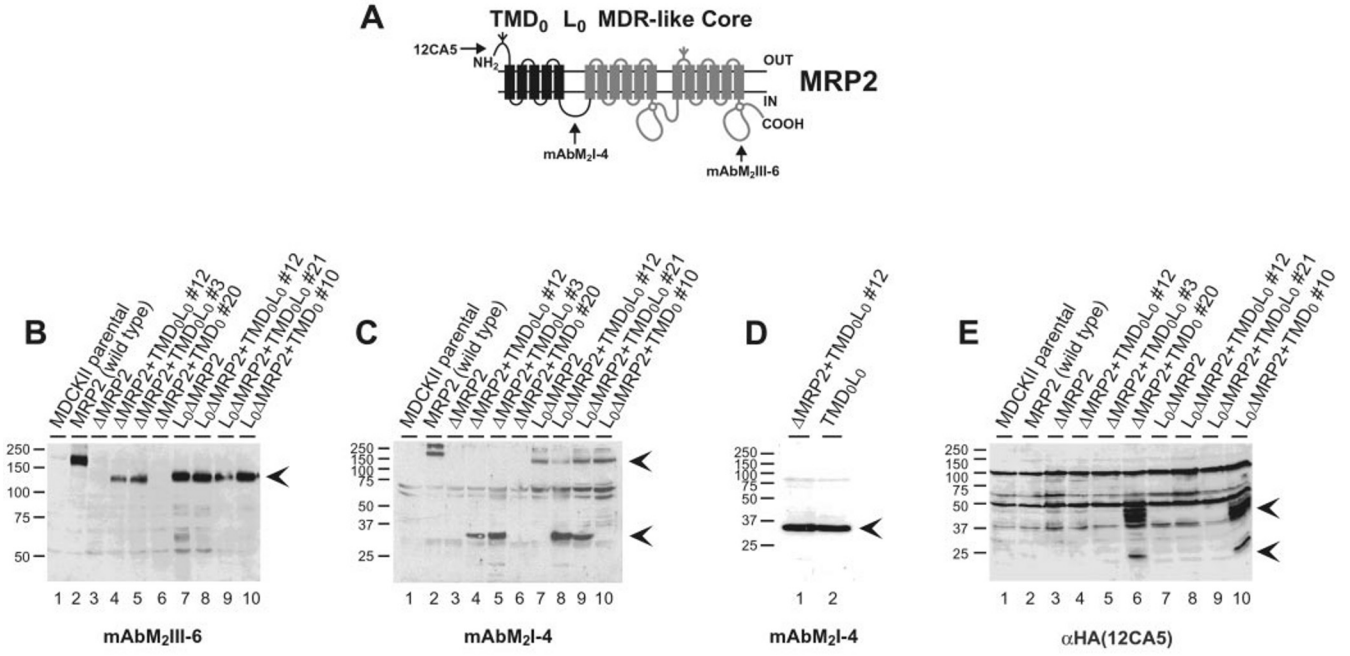

FIG. 2. **Detection of MRP2 variants in MDCKII cells by Western blot analysis.** *A*, schematic representation of MRP2. The regions recognized by the mAbs used are indicated. *B–E*, Western blot analysis with total cell lysates from MDCKII-derived clones. 20 μg of protein was size-fractionated in a 7.5% (*B*) or 11% (*C–E*) denaturing polyacrylamide gel. After immunoblotting, MRP2 fragments were visualized with mAbs M_2III-6 (*B*), M_2I-4 (*C* and *D*), or 12CA5 (*E*). The relevant protein bands are marked with *arrows*. Protein-antibody interactions were detected using the enhanced chemiluminescence technique.

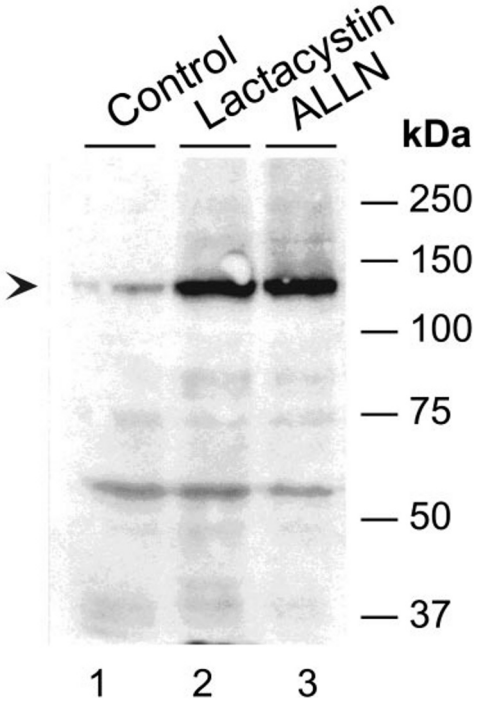

FIG. 3. **Effect of proteasome inhibitors on the degradation of ΔMRP2.** MDCKII-ΔMRP2 cells were treated without inhibitor (*lane 1*), lactacystin (50 μM; *lane 2*), or ALLN (50 μg/ml; *lane 3*). Cells were incubated with inhibitors for 8 h. Cell lysates (20 μg) were size-fractionated in a 7.5% polyacrylamide gel (see Fig. 2). ΔMRP2 was detected with mAb M_2III-6.

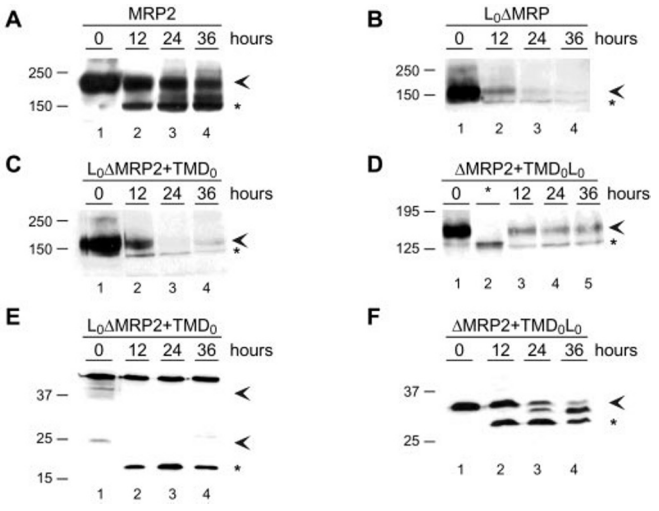

FIG. 4. **Tunicamycin treatment of MDCKII-derived clones.** Cells were treated with tunicamycin (1.5 μg/ml) for 0, 12, 24, or 36 h. Lysates were size-fractionated in 7.5% (*A–D*) or 11% (*E* and *F*) polyacrylamide gels. Blots were incubated with mAbs M_2III-6 (*A–D*), 12CA5 (*E*), or M_2I-4 (*F*). The *lane* marked with an *asterisk* in *D* (*lane 2*) contains a lysate from MDCKII-ΔMRP2 cells treated with lactacystin. *Arrows*, glycosylated proteins; *stars*, deglycosylated proteins.

$TMD_0L_0\Delta$ protein were isolated. Remarkably, whereas ΔMRP2 produced alone was hardly detectable, co-production with TMD_0L_0 resulted in a strong increase in the amount of ΔMRP2 (Fig. 2*B*, *lane 3 versus lanes 4* and *5*). In the clone containing both ΔMRP2 and TMD_0 (without the L_0 part), the amount of ΔMRP2 was not increased (Fig. 2*B*, *lane 6*). Cells producing $L_0\Delta$MRP2 and TMD_0L_0 or TMD_0, respectively, were also isolated (Fig. 2, *C* and *E*, *lanes 8–10*). In these clones, no significant changes in the level of $L_0\Delta$MRP2 were observed (Fig. 2*B*). TMD_0 appeared as a discrete band with an apparent molecular mass of 24 kDa and a number of bands around 40 kDa (Fig. 2*E*, *lanes 6* and *10*). These are most likely explained by differential glycosylation as shown below. Whereas clones producing the TMD_0L_0 region alone were isolated (Fig. 2*D*, *lane 2*), we only detected TMD_0 if it was combined with ΔMRP2 (Fig. 2*E*, *lane 6*) or $L_0\Delta$MRP2 (Fig. 2*E*, *lane 10*).

The glycosylation sites present in MRP2 have not been mapped but, like in MRP1 (35), *N*-glycosylation sequences are

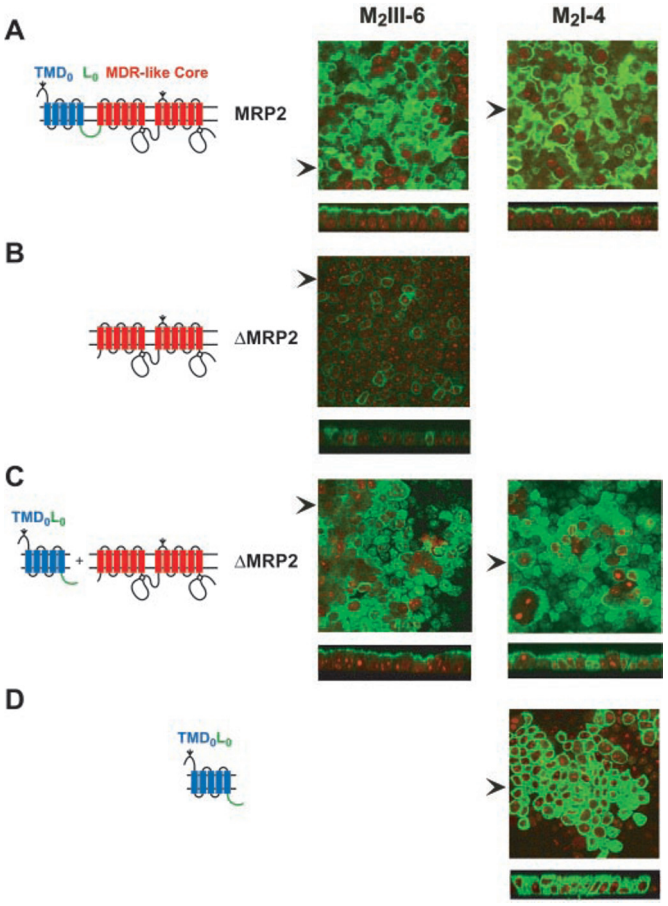

FIG. 5. **Immunolocalization by confocal laser-scanning microscopy of MRP2 and ΔMRP2 plus N-terminal fragments in MDCKII monolayers.** *A*, wild-type MRP2; *B*, ΔMRP2; *C*, TMD_0L_0 plus ΔMRP2; *D*, TMD_0L_0. The various proteins were detected by indirect immunofluorescence (*green signal*) with mAb M_2III-6 or M_2I-4. Antibody-antigen interactions were detected with a fluorescein isothiocyanate-labeled secondary antibody. Nucleic acids were detected by counterstaining with propidium iodide (*red signal*). The *upper part* of each *panel* shows a top (*x/y*) view of the cell monolayer; the *lower part* shows a vertical (*x/z*) section. The constructs stably expressed in the various cell lines are indicated on the *left sides* of the *panels*. The *arrows* indicate the position where the *x/z* section was made.

present in the N terminus (amino acids 7 and 12) and between putative transmembrane segments 12 and 13 (amino acid 1011). To investigate whether the various fragments of MRP2 were glycosylated, cells were grown in the presence of tunicamycin, a drug preventing *N*-linked glycosylation. As expected, full-length MRP2 was glycosylated as illustrated by the appearance of a smaller band, around 150 kDa in the presence of tunicamycin (Fig. 4*A*). L_0ΔMRP2 was glycosylated both in the presence and absence of TMD_0 (Fig. 4, *B* and *C*). Part of ΔMRP2 was core-glycosylated if produced alone, as illustrated by the band visible just above the unglycosylated protein (Fig. 4*D*, *lane 2*). Interestingly, ΔMRP2 became fully glycosylated if coproduced with the TMD_0L_0 polypeptide, and this glycosylation was inhibited by treatment with tunicamycin (Fig. 4*D*). The amounts of unglycosylated MRP2, L_0ΔMRP2, and ΔMRP2 were strongly reduced compared with the glycosylated forms, suggesting that the unglycosylated proteins are rapidly degraded. Both the TMD_0 and TMD_0L_0 fragments were also glycosylated. An increased mobility of these proteins was observed in the presence of tunicamycin (Fig. 4, *E* and *F*). For MRP2 and TMD_0L_0, intermediate bands were observed between the glycosylated and deglycosylated proteins after $t = 24$ and 36 h (Fig. 4, *A* and *F*, *lanes 3* and *4*). These could either be due to proteolysis or partial deglycosylation by endogenous endoglycosidases.

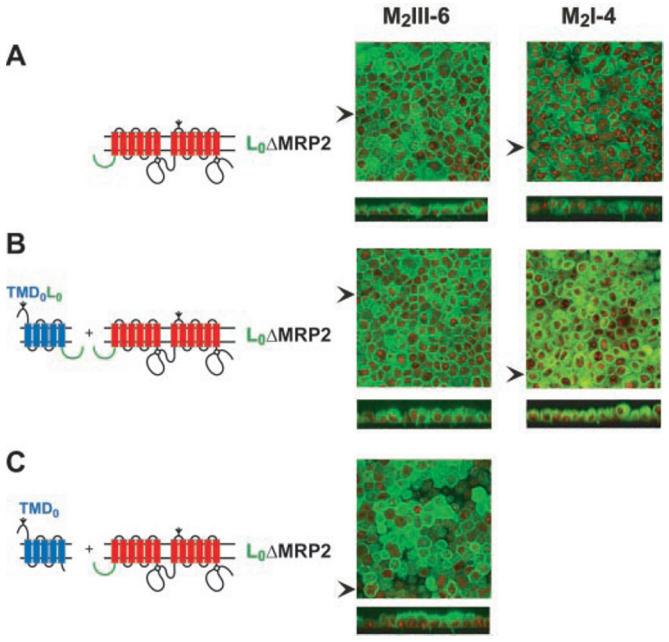

FIG. 6. **Immunolocalization of L_0ΔMRP2 and N-terminal fragments in MDCKII-derived monolayers.** *A*, L_0ΔMRP2; *B*, TMD_0L_0 plus L_0ΔMRP2; *C*, TMD_0 plus L_0ΔMRP2. For details, see the legend to Fig. 5.

Immunolocalization of MRP2 Mutants in MDCKII Monolayers—The subcellular localization of the various MRP2 mutants was determined by indirect immunofluorescence using confocal laser-scanning microscopy. The proteins were detected with the same mAbs as used in the Western blot experiments. Cells were analyzed at the horizontal plane (*x/y*) and at the plane perpendicular to the monolayer (*x/z*). The apically localized wild-type MRP2 was used as a control in these experiments (Fig. 5*A*). The results for ΔMRP2 can be summarized as follows: (i) ΔMRP2 alone was present in low concentrations in an intracellular compartment, probably the endoplasmic reticulum, but we have not verified this (Fig. 5*B*). (ii) ΔMRP2 in cells co-expressing TMD_0L_0 together with ΔMRP2 was mainly present in the apical membrane (Fig. 5*C*). A substantial amount of the TMD_0L_0 protein was localized intracellularly. Some protein, however, was also detected in the apical membrane. (iii) ΔMRP2 was detected intracellularly in cells co-expressing ΔMRP2 and TMD_0 (data not shown). (iv) The TMD_0L_0 polypeptide alone was localized in an intracellular compartment (Fig. 5*D*).

Since we previously found that L_0ΔMRP1 was properly routed to the lateral membrane, we investigated whether L_0ΔMRP2 similarly routed to the apical membrane. The results shown in Fig. 6 document the following. (i) The L_0ΔMRP2 protein produced alone is localized intracellularly (Fig. 6*A*). (ii) In cells co-expressing L_0ΔMRP2 and TMD_0, the L_0ΔMRP2 protein was in the apical membrane, although some intracellular staining was also observed (Fig. 6*C*). In these cells, we could not visualize the TMD_0 polypeptide with mAb 12CA5 in immunofluorescence experiments. Full-length, HA-tagged MRP2 was also not detectable by immunofluorescence, although the protein was functional and visualized in Western blots with mAb 12CA5 (data not shown). The HA epitope is probably not accessible in these proteins, since we also did not succeed in detecting it with other anti-HA mAb or polyclonal antibodies using different fixation methods. (iii) In cells co-expressing L_0ΔMRP2 and TMD_0L_0, both proteins were detected intracellularly (Fig. 6*B*). Taken together, these data suggest that the

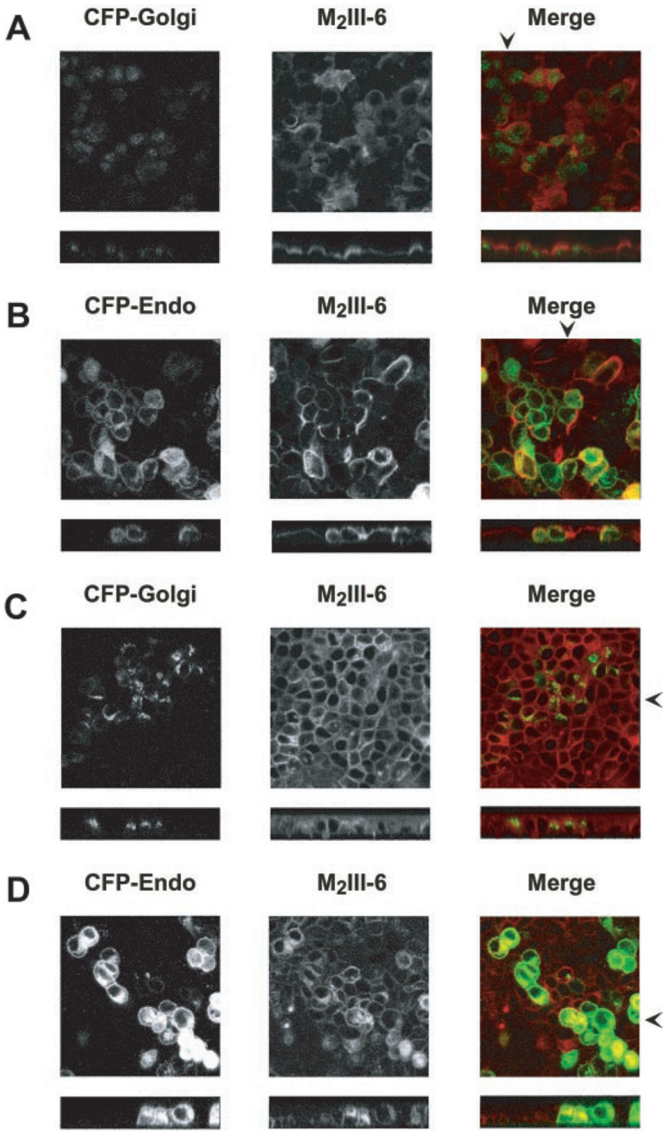

FIG. 7. **Co-localization of L_0ΔMRP2 with the ECFP-Endo and ECFP-Golgi proteins in MDCKII-MRP2 and MDCKII-L_0ΔMRP2 cells.** After fixing the cells, MRP2 (*A* and *B*) and L_0ΔMRP2 (*C* and *D*) were detected by indirect immunofluorescence using mAb M_2III-6 and Alexa 532. The *left panels* show the signal obtained with mAb M_2III-6, and the *middle panels* show the ECFP signal detected with pECFP-Golgi (*A* and *C*) and pECFP-Endo (*B* and *D*). The merge of the Alexa 532 (in *red*) and ECFP signals (in *green*) is shown in the *panels* on the *right*. Co-localization of both proteins is represented by a *yellow signal*. An *arrow* indicates the position where the *x/z* section was made.

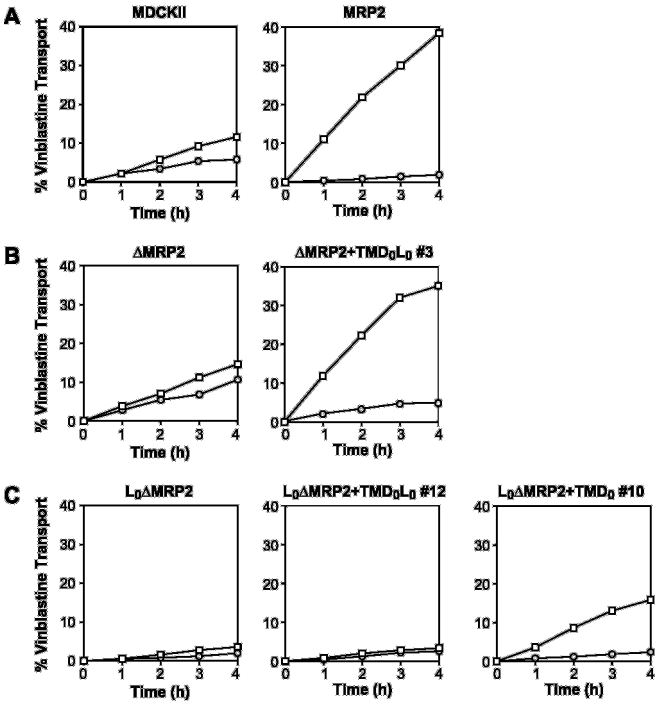

FIG. 8. **Vectorial transport of [^{3}H]vinblastine by MDCKII-derived monolayers.** *A–C*, at $t = 0$, [^{3}H]vinblastine (2 μM) was applied either in the apical or in the basal compartment, and the percentage of radioactivity appearing in the opposite compartment was determined. Transport is presented as the fraction of radioactivity added at the beginning of the experiment, appearing in the opposite compartment. PSC833 (0.1 μM) was present in both compartments to inhibit the endogenous MDR1 Pgp present in these cells. *Squares*, translocation from basal to apical. *Circles*, translocation from apical to basolateral. The experiments were performed in duplicate and repeated three times. A typical experiment is shown.

TMD_0 and TMD_0L_0 polypeptides interact with L_0ΔMRP2 and ΔMRP2, respectively, to form a protein routed to the apical membrane.

Since L_0-MRP2 is glycosylated, it most likely is not a folding mutant associated with the endoplasmic reticulum. To analyze whether the protein was associated with endosomes or the Golgi apparatus, we performed co-localization studies with fluorescently labeled marker proteins. As marker for the Golgi apparatus, we used a fusion protein consisting of ECFP and a sequence encoding the N-terminal 81 amino acids of human β-1,4-galactosyltransferase (pECFP-Golgi) (36). As a marker for endosomes, we used the pECFP-Endo vector, which encodes a fusion protein between ECFP and the human RhoB GTPase (37). Stable MDCKII-MRP2 and MDCKII-L_0ΔMRP2 cells were transiently transfected with the pECFP constructs. The co-localization of proteins in these assays resulted in a yellow signal after merging the ECFP signal (shown in *green* in Fig. 7, *left panels*) with the signal obtained with mAb M_2III-6 (shown in *red*, *middle panels*). No overlap was detected between MRP2 and the ECFP-Golgi protein, whereas some overlap was found between MRP2 and the ECFP-Endo protein (Fig. 7, *A* and *B*, *right panels*). Like MRP2, L_0ΔMRP2 was not co-localizing with the ECFP-Golgi marker (Fig. 7*C*), but overlap was found in the merge with the pECFP-Endo marker (Fig. 7*D*), suggesting that at least part of this protein is associated with endosomes.

Transport of [^{3}H]Vinblastine and [^{14}C]Dinitrophenyl Glutathione by MDCKII-derived Monolayers—To verify whether the co-produced proteins detected in the apical membrane were properly folded, we tested their biological activity. We have shown that wild-type MRP2 is able to transport the *Vinca* alkaloid [^{3}H]vinblastine to the apical side of a cell monolayer (11, 30). Using the same assay conditions, we analyzed the transport of vinblastine by the MDCKII-derived cell lines expressing the various regions of MRP2. Fig. 8*A* shows that wild-type MDCKII cells transported little vinblastine under the experimental conditions employed, whereas MDCKII-MRP2 cells demonstrated a clearly increased transport of vinblastine to the apical side of the cell monolayer. Neither in MDCKII-L_0ΔMRP2 nor in MDCKII-ΔMRP2 cells was a significantly increased transport rate detected to either side of the monolayer. In contrast, transport to the apical side of the monolayer was clearly increased in cells co-expressing ΔMRP2 and TMD_0L_0 or co-expressing L_0ΔMRP2 and TMD_0, respectively (Fig. 8, *B* and *C*, *right versus left panels*).

An important characteristic of MRP2 is its ability to transport certain organic anions. A model substrate to measure MRP-mediated transport of an organic anion from intact cells is DNP-GS. DNP-GS is hydrophilic and therefore only slowly

TABLE I

Transport into the medium, intracellular accumulation, and total synthesis of [^{14}C]DNP-GS by MDCKII-derived monolayers after incubation for 20 min with [^{14}C]CDNB

Transport of DNP-GS by MDCKII-derived monolayers. At $t = 0$, [^{14}C]CDNB (final concentration 2 μM; 15 nCi ml^{-1}) was added to the apical and basal compartment. Samples were taken at $t = 1$, 3, 6, 12, and 20 min and extracted with ethyl acetate to separate DNP-GS from unconjugated CDNB. Values presented represent the total amount of [^{14}C]DNP-GS (in pmol) transported in the apical or basal medium after 20 min. "Intracellular" represents the amount of radioactivity associated with the cells, and "Total" represents the sum of the total amount of DNP-GS transported into the medium and detected intracellularly. The experiments were performed twice in duplicate. A typical experiment is shown, and the variation between the measurements is indicated.

Cell line	DNP-GS transport (in pmoles per monolayer)			
	Apical	Basal	Intracellular	Total
	pmol/monolayer			
MDCKII	423 ± 38	706 ± 18	575 ± 74	1704
MRP2	1377 ± 110	436 ± 60	343	2156
ΔMRP2	375 ± 9	701 ± 86	342 ± 6	1418
ΔMRP2 + TMD_0L_0# 12	670 ± 47	832 ± 9	242 ± 17	1744
ΔMRP2 + TMD_0L_0# 3	922 ± 147	800 ± 164	304 ± 43	2026
L_0ΔMRP2	239 ± 25	904 ± 57	449 ± 60	1592
L_0ΔMRP2 + TMD_0L_0# 12	164 ± 11	925 ± 180	362 ± 16	1451
L_0ΔMRP2 + TMD_0L_0# 21	216 ± 67	730 ± 185	490 ± 112	1436
L_0ΔMRP2 + TMD_0# 10	592 ± 69	507 ± 111	175 ± 7	1274

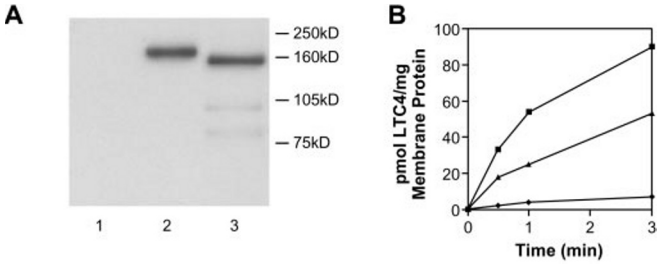

FIG. 9. **Functional analysis of L_0ΔMRP2 in baculovirus-infected Sf9 cells.** *A*, Western blot of Sf9 cell membranes containing β-galactosidase (*lane 1*), MRP2 (*lane 2*), and L_0ΔMRP2 (*lane 3*). The proteins were detected with mAb M_2III-6. *B*, ATP-dependent uptake of LTC_4 in Sf9 vesicles containing MRP2 (*squares*), L_0ΔMRP2 (*triangles*), or β-galactosidase (*diamonds*). Membrane preparations were incubated with LTC_4 (240 nM) at 23 °C. ATP-dependent uptake was calculated by subtracting the values obtained in the presence of 4 mM AMP from those in the presence of 4 mM ATP. Samples were taken at $t = 0.5$, 1, and 3 min.

diffuses over the plasma membrane. To measure transport of this compound, cells are incubated with the hydrophobic precursor [^{14}C]CDNB. This compound rapidly diffuses across membranes and is conjugated intracellularly to glutathione by glutathione *S*-transferases. The [^{14}C]DNP-GS formed can only leave the cells via an active transporter (38). As shown before, apical DNP-GS transport by MDCKII-MRP2 monolayers was 3.2-fold higher than in the wild type cells (Table I). In MDCKII-L_0ΔMRP2 monolayers, the apical transport activity was 1.8-fold lower than in wild-type cells. This might be due to a down-regulation of the endogenous canine MRP2 that is present in these cells (11). Basolateral transport of DNP-GS was somewhat variable among the different clones, probably due to variation in expression levels of endogenous basolaterally localized organic anion transporters. This variation did not correlate with the expression of MRP2 variants. In two clones tested, co-expression of ΔMRP2 with TMD_0L_0 resulted in a 1.8–2.5-fold higher apical transport of DNP-GS than in cells containing ΔMRP2 alone. Co-expression of L_0ΔMRP2 with TMD_0L_0 did not result in an increased transport to the apical side of the monolayer. In contrast, apical transport was increased 2.5-fold in the cells containing both L_0ΔMRP2 and TMD_0, compared with cells producing L_0ΔMRP2 alone.

Taken together, these data show a correlation between the presence of L_0ΔMRP2 plus TMD_0 and ΔMRP2 plus TMD_0L_0, respectively, in the apical membrane and transport of both vinblastine and DNP-GS.

Uptake of LTC_4 in Membrane Vesicles Containing L_0ΔMRP2—The experiments shown above indicate that L_0ΔMRP2 did not transport drugs into the medium in MDCKII cells and was localized intracellularly. To investigate whether L_0ΔMRP2 is able to transport leukotriene C_4, a typical substrate for MRP2, we expressed MRP2 and L_0ΔMRP2 in baculovirus-infected insect (Sf9) cells. Fig. 9*A* shows that we obtained similar levels of MRP2 and L_0ΔMRP2 in membrane vesicles prepared from these cells. To examine the functionality of L_0ΔMRP2, ATP-dependent uptake of LTC_4 was determined in isolated membrane vesicles. The apparent transport rate of L_0ΔMRP2 for LTC_4 (240 nm) was ~50% of the transport of wild-type MRP2 (Fig. 9*B*). These transport rates were corrected for the differences in protein levels and for the transport-competent inside-out vesicles content, as determined by measuring active Ca^{2+} uptake. The transport rate of L_0ΔMRP2, measured in the presence of higher concentrations of LTC4 (720 nM) for 30 s, was also found to be about 50% of wild type MRP2, indicating that deletion of the TMD_0 region did not cause a major change in the apparent K_m of L_0ΔMRP2 for LTC_4.

DISCUSSION

By co-expressing various mutants of MRP2 in polarized MDCKII cells, we searched for regions that are important for routing of MRP2 to the apical plasma membrane. In MDCKII cells, the L_0ΔMRP2 protein was localized intracellularly and mainly associated with endosomes. Uptake experiments with L_0ΔMRP2-containing vesicles that were isolated from baculovirus-infected Sf9 cells demonstrated that this mutant protein is in principle functional, since it mediated the transport of the MRP2 substrate LTC_4. Co-expression in MDCKII cells of the N-terminal fragments TMD_0L_0 and TMD_0 with the core fragments ΔMRP2 and L_0ΔMRP2, respectively, resulted in routing to the apical plasma membrane. Co-produced mutants localized in the apical membrane are functional, since they transport both the *Vinca* alkaloid vinblastine and the organic anion DNP-GS. This strongly suggests that the co-produced MRP2 fragments are properly folded and that routing is most likely determined by the same signals that are functional in wild-type MRP2. Our data suggest that the complete TMD_0L_0 region of MRP2 is required for routing, although it is also possible that TMD_0L_0 is required to remain stably localized in the apical membrane. These findings are in contrast to our previous experiments with MRP1 mutants, which showed that the TMD_0 region of MRP1 is not required for routing to the lateral membrane (27, 28).

In cells producing ΔMRP2 and TMD_0L_0, only a fraction of the latter protein was detectable in the apical membrane, whereas all ΔMRP2 was in the apical membrane. We hypothesize that the TMD_0L_0 region is required for the sorting of ΔMRP2 from the ER to the Golgi apparatus, where it becomes glycosylated. The TMD_0L_0 protein probably is expressed in molar excess in our cells, resulting in routing of only those TMD_0L_0 molecules that interact with ΔMRP2. This hypothesis is in line with the observation that TMD_0L_0 in the absence of ΔMRP2 is localized intracellularly.

The ΔMRP2 protein in the absence of TMD_0L_0 is most likely degraded by proteasomes, since the protein was only detectable at very low concentrations and was only core-glycosylated. Moreover, treatment with two different proteasome inhibitors resulted in a substantially increased amount of the protein. Co-expression with TMD_0L_0 clearly increased the stability of ΔMRP2 and resulted in glycosylation. These findings are not specific for ΔMRP2, since we found the same in cells containing ΔMRP1 and its N-terminal TMD_0L_0 fragment.[2] We do not know at present whether ΔMRP2 is a misfolded protein and therefore recognized by the quality control system of the cell, resulting in proteasome-mediated degradation, or whether this molecule lacks signals that are required for sorting from the ER to the Golgi apparatus. Such signals should then be present in L_0, since the L_0ΔMRP2 protein is glycosylated and functional, at least *in vitro*. Remarkably, the L_0ΔMRP2 mutant was glycosylated in the absence of TMD_0 but was not detected in the plasma membrane.

L_0ΔMRP2 was in part co-localizing with the ECFP-Endo and not with the ECFP-Golgi protein. An interesting question is whether L_0ΔMRP2 is routed from the Golgi apparatus to the plasma membrane and subsequently rapidly endocytosed or directly sorted from the Golgi to endosomes. The implication of the former hypothesis is that TMD_0 is required for MRP2 to remain stably localized in the apical membrane. Alternatively, it is tempting to speculate that TMD_0 is required for routing of L_0ΔMRP2 and that this region contains an apical routing signal. At steady state, however, we see only intracellular staining of the TMD_0L_0 protein produced alone. This indicates that a possible routing signal only functions in the context of the complete molecule.

It is possible that MRP2 contains multiple signals required for routing. That routing signals in polytopic apically localized transporters may be complex is illustrated by recent experiments in which the routing behavior of chimeric proteins containing part of the Na/K-ATPase α-subunit (basolateral localization) and the H,K-ATPase α-subunit (apical localization) was studied (39). Both the extracellular and intracellular loops flanking transmembrane segment four of the H,K-ATPase, but not transmembrane four itself, were sufficient to redirect the normally basolaterally localized Na,K-ATPase to the apical membrane. Following a similar approach for MRP1 and MRP2 may be difficult, since most of the chimeric molecules we analyzed remained associated with the endoplasmic reticulum.[3]

Another ATP binding cassette transporter that shows some structural homology to MRPs is the cystic fibrosis transmembrane conductance regulator (CFTR). The C terminus of CFTR contains sequences important for routing to the apical membrane. The last three C-terminal amino acids form a PDZ-binding motif that interacts with proteins containing PDZ domains (40, 41). Interestingly, a CFTR with a truncation of the last three amino acids had lost its apical localization and was distributed between the apical and basolateral membrane (42). Subsequent work showed that additional C-terminal residues are required for localizing CFTR to the apical membrane (43). As one of the PDZ domain-containing proteins, PDZK1 (also called CAP1), which binds to CFTR, also interacts with the C terminus of MRP2 (43), it has been speculated that PDZ domain-containing proteins play a role in the localization of MRP2 (45). Although we formally cannot exclude the possibility that sequences present in the C-terminal tail of MRP2 play an additional role in routing, the last three amino acids are not required in the MDCKII cell line we use, since an MRP2 mutant lacking these last three amino acids localizes to the apical membrane and is functional.[4] For the time being, we have no evidence that MRP2 contains routing information in another region than in TMD.

Acknowledgments—We thank G. Calenda, C. Shemanko, S. Theis, and M. Zörnig for critical comments on the manuscript. We gratefully acknowledge Drs. M. Kneussel and H. Betz (Max-Planck Institute for Brain Research, Frankfurt) for use of the confocal laser-scanning microscope, Dr. R. Scheper and G. Scheffer (Free University Hospital, Amsterdam) for providing the anti-MRP2 monoclonal antibodies, Dr. J. Collard (Netherlands Cancer Institute, Amsterdam) for providing the 12CA5 antibody, and Dr. R. Oude Elferink (Academic Medical Center, Amsterdam) for providing [^{14}C]CDNB. We also thank M. McColgan for artwork.

REFERENCES

1. Juliano, R. L., and Ling, V. (1976) *Biochim. Biophys. Acta* **455,** 152–162
2. Cole, S. P. C., Bhardwaj., G., Gerlach, J. H., Mackie, J. E., Grant, C. E., Almquist, K. C., Stewart, A. J., Kurz, E. U., Duncan, A. M. V., and Deeley, R. G. (1992) *Science* **258,** 1650–1654
3. Paulusma, C. C., Bosma, P. J., Zaman, G. J. R., Bakker, C. T. M., Otter, M., Scheffer, G. L., Scheper, R. J., Borst, P., and Oude Elferink, R. P. J. (1996) *Science* **271,** 1126–1128
4. Ambudkar, S. V., Dey, S., Hrycyna, C. A., Ramachandra, M., Pastan, I., and Gottesman M. M. (1999) *Annu. Rev. Pharmacol. Toxicol.* **39,** 361–398
5. Leier, I., Jedlitschky, G., Buchholz, U., Cole, S. P. C., Deeley, R. G., and Keppler, D. (1994) *J. Biol. Chem.* **269,** 27807–27810
6. Jedlitschky, G., Leier, I., Buchholz, U., Barnouin, K., Kurz, G., and Keppler, D. (1996) *Cancer Res.* **56,** 988–994
7. König, J., Nies, A., Cui, Y., Leier, I., and Keppler, D. (1999) *Biochim. Biophys. Acta* **1461,** 377–394
8. Rappa, J., Lorico, A., Flavell, R. A., and Sartorelli, A. C. (1997) *Cancer Res.* **57,** 5232–5237
9. Loe, D. W., Deeley, R. G., and Cole, S. P. C. (1998) *Cancer Res.* **58,** 5130–5136
10. Renes, J., de Vries, E. G., Nienhuis, E. F., Jansen, P. L., and Muller, M. (1999) *Br. J. Pharmacol.* **126,** 681–688
11. Evers, R., de Haas, M., Sparidans, R., Beijnen, J., Wielinga, P. R., Lankelma, J., and Borst P. (2000) *Br. J. Cancer* **83,** 375–383
12. Mao, Q., Deely, R. G., and Cole, S. P. C. (2000) *J. Biol. Chem.* **275,** 34166–34172
13. Kool, M., de Haas, M., Scheffer, G. L., Scheper, R. J., van Eijk, M. J. T., Juijn, J. A., Baas, F., and Borst, P. (1997) *Cancer Res.* **57,** 3527–3547
14. Hopper, E., Belinsky, M. G., Zeng, H., Tosolini, A., Testa, J. R., and Kruh, G. D. (2001) *Cancer Lett.* **162,** 181–191
15. Bera, T. K., Lee, S., Salvatore, G., Lee, B., and Pastan, L. (2001) *Mol. Med.* **7,** 509–516
16. Hirohashi, T., Suzuki, H., and Sugiyama, Y. (1999) *J. Biol. Chem.* **274,** 15181–15185
17. Zeng, H., Bain, L. J., Belinski, M. G., and Kruh, G. D. (1999) *Cancer Res.* **59,** 5964–5967
18. Kool, M., van der Linden, M., de Haas, M., Scheffer, G. L., de Vree, J. M. L., Smith, A. J., Janssen, G., Peters, G. J., Ponne, N., Scheper, R. J., Oude Elferink, R. P. J., and Borst, P. (1999) *Proc. Natl. Acad. Sci. U. S. A.* **96,** 6914–6919
19. Schuetz, J. D., Connelly, M. C., Sun, D., Paibir, S. G., Flynn, P. M., Srinivas, R. V., Kumar, A., and Fridland, A. (1999) *Nat. Med.* **5,** 1048–1051
20. Wijnholds, J., Mol, C. A. A. M., van Deemter, L., de Haas, M., Scheffer, G. L., Baas, F., Beijnen, J. H., Scheper, R. J., Hatse, S., De Clercq, E., Balzarini, J., and Borst, P. (2000) *Proc. Natl. Acad. Sci. U. S. A.* **97,** 7476–7481
21. Lee, K., Klein-Szanto, A. J., and Kruh, G. D. (2000) *J. Natl. Cancer Inst.* **6,** 1934–1940
22. Bakos, E., Klein, I., Welker, E., Szabo, K., Muller, M., Sakardi, B., Varadi, A. (1996) *Biochem. J.* **323,** 777–783
23. Hipfner, D. R., Gao, M., Scheffer, G., Scheper, R. J., Deeley, R. G., and Cole, S. P. (1998) *Br. J. Cancer* **78,** 1134–1140
24. Gao, M., Yamazaki, M., Loe, D. W., Westlake, C. J., Grant, C. E., Cole, S. P. C., and Deeley, R. G. (1998) *J. Biol. Chem.* **273,** 10733–10740
25. Kast, C., and Gros, P. (1997) *J. Biol. Chem.* **272,** 26479–26487
26. Klein, I., Sarkadi, B., and Varadi, A. (1999) Biochem. *Biophys. Acta* **1461,** 237–262
27. Bakos, E., Evers, R., Szacacs, G., Tusnady, G. E., Welker, E., Szabo, K., de Haas, M., van Deemer, L., Borst, P., Varadi, A., and Sakardi, B. (1998)

[2] G. Calenda and R. Evers, unpublished data.
[3] R. Evers and P. Borst, unpublished observations.
[4] S. B. M. Fernández and R. Evers, unpublished results.

J. Biol. Chem. **273,** 32167–321675
28. Bakos, E., Evers, R., Calenda, G., Tusnady, G. E., Szakacs, G., Varadi, A., and Sarkadi, B. (2000) *J. Cell Sci.* **113,** 4451–4461
29. Evers, R., Cnubben, N. H., Wijnholds, J., van Deemter, L., van Bladeren, P. J., and Borst, P. (1997) *FEBS Lett.* **419,** 112–116
30. Evers, R., Kool, M., van Deemter, L., Janssen H., Calafat, J., Oomen, L. C. J. M., Paulusma, C. C., Oude Elferink, R. P. J., Baas, F., Schinkel, A. H., and Borst, P. (1998) *J. Clin. Invest.* **101,** 1310–1319
31. Cui, Y., Buchholz, J. K., Spring, H., Leier, I., and Keppler, D. (1999) *Mol. Pharmacol.* **55,** 929–937
32. Paulusma, C. C., Kool, M., Bosma, P. J., Scheffer, G. L., ter Borg, F., Scheper, R. J., Borst, P., Baas, F., and Oude Elferink, R. P. J. (1997) *Hepatology* **25,** 1539–1542
33. Bengal, E., Ransone, L., Scharfman, R., Dwarki, R., Tapscott, S. J., Weintraub, H., and Verma, I. M. (1992) *Cell* **68,** 507–519
34. Scheffer, G. L., Kool, M., Heijn, M., de Haas, M., Pijnenborg, A. C., Wijnholds, J., van Helvoort, A., de Jong, M. C., Hooijberg, J. H., Mol, C. A., van der Linden, M., de Vree, J. M., van der Valk, P., Elferink, R. P., Borst, P., and Scheper, R. J. (2000) *Cancer Res.* **60,** 5269–5277
35. Hipfner, D. R., Almquist, K. C., Leslie, E. M., Gerlach, J. H., Grant, C. E., Deely, R. G., Cole, S. P. C. (1997) *J. Biol. Chem.* **272,** 23623–23630
36. Llopis, J., McCaffery, J. M., Miyawaki, A., Farquhar, M. G., and Tsien, R. Y. (1998) *Proc. Natl. Acad. Sci. U. S. A.* **95,** 6803–6808
37. Adamson, P., Paterson, H. F., Hall, A. (1992) *J. Cell Biol.* **119,** 617–627
38. Oude Elferink, R. P. J., Bakker, C. T. M., and Jansen, P. L. M. (1993) *Biochem. J.* **290,** 759–764
39. Dunbar, L. A., Aronson, P., and Caplan, M. J. (2000) *J. Cell Biol.* **148,** 769–778
40. Moyer, B. D., Duhaime, M., Shaw, C., Denton, J., Reynolds, D., Karlson, K. H., Pfeiffer, J., Wang, S., Mickle, J. E., Milewski, M., Cutting, G. R., Guggino, W. B., Li, M., and Stanton, B. A. (2000) *J. Biol. Chem.* **275,** 27069–27074
41. Kleizen, B., Braakman, I., and de Jong, H. (2000) *Eur. J. Cell Biol.* **79,** 544–556
42. Moyer, B. D., Denton, J., Karlson, K. H., Reynolds, D., Wang, S., Mikle, J. E., Milewski, M., Cutting, G. R., Guggino, W. B., Li, M., and Stanton, B. A. (1999) *J. Clin. Invest.* **104,** 1353–1361
43. Milewski, M. I., Mickle, J. E., Forrest, J. K., Stafford, D. M., Moyer, B. D., Cheng, J., Guggino, W. B., Stanton, B. A., and Cutting, G. R. (2001) *J. Cell Science* **114,** 719–726
44. Kocher, O., Comella, N., Gilchrist, A., Pal., R., Tognazzi, K., Brown, L. F., and Knoll, J. H. M. (1999) *Lab. Invest.* **79,** 1161–1170
45. Harris, M. J., Kuwano, M., Webb, M., Board, P. G. (2001) *J. Biol. Chem.* **24,** 20876–20881